

# Dispersion relations and Unitary Isobar Model in single pion electro-production; low and high $Q^2$

I. G. Aznauryan

Jefferson Lab  
Yerevan Physics Institute

May 26, 2010, JLab

Using DR and UIM we have analysed all JLab-CLAS pion electro-production data in the  $P_{33}(1232)$  and  $P_{11}(1440)$ ,  $D_{13}(1520)$ , and  $S_{11}(1535)$  resonance regions available today at  $Q^2=0.16-4.5 \text{ GeV}^2$ : PR C80,055203 (2009)

**1.** chi2 were approximately the same in both approaches

**2.** All model uncertainties were taken into account:

uncertainties of the background contributions related to the form factors in the Born term and  $\rho$  and  $\omega$  contributions

uncertainties due to higher resonance contributions

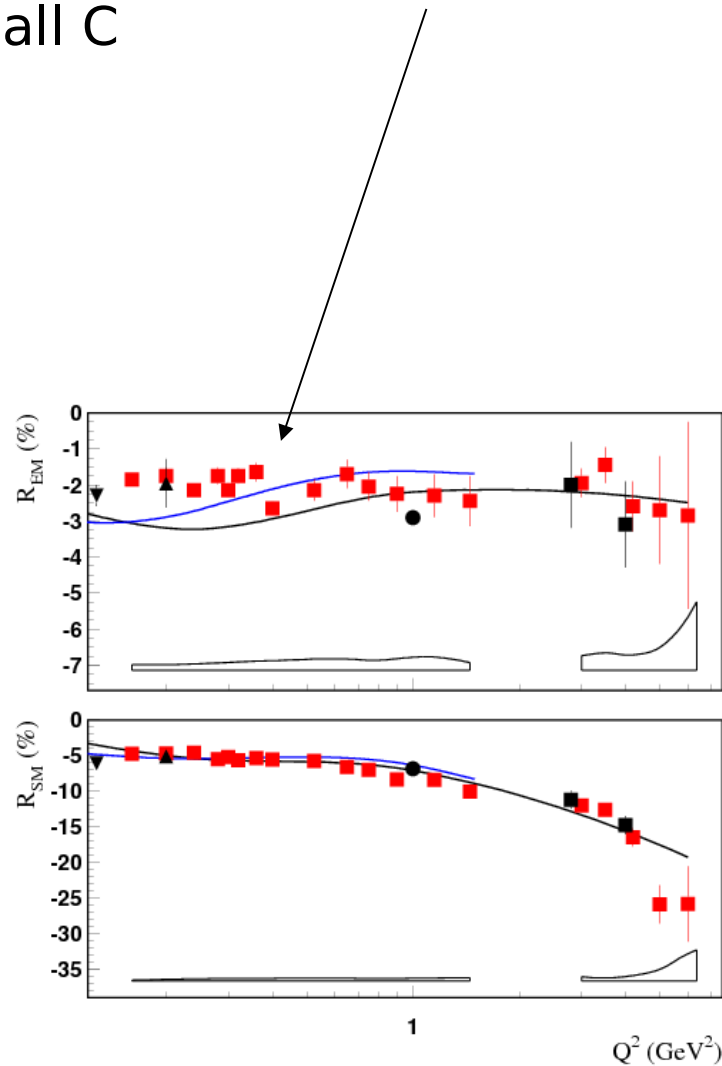
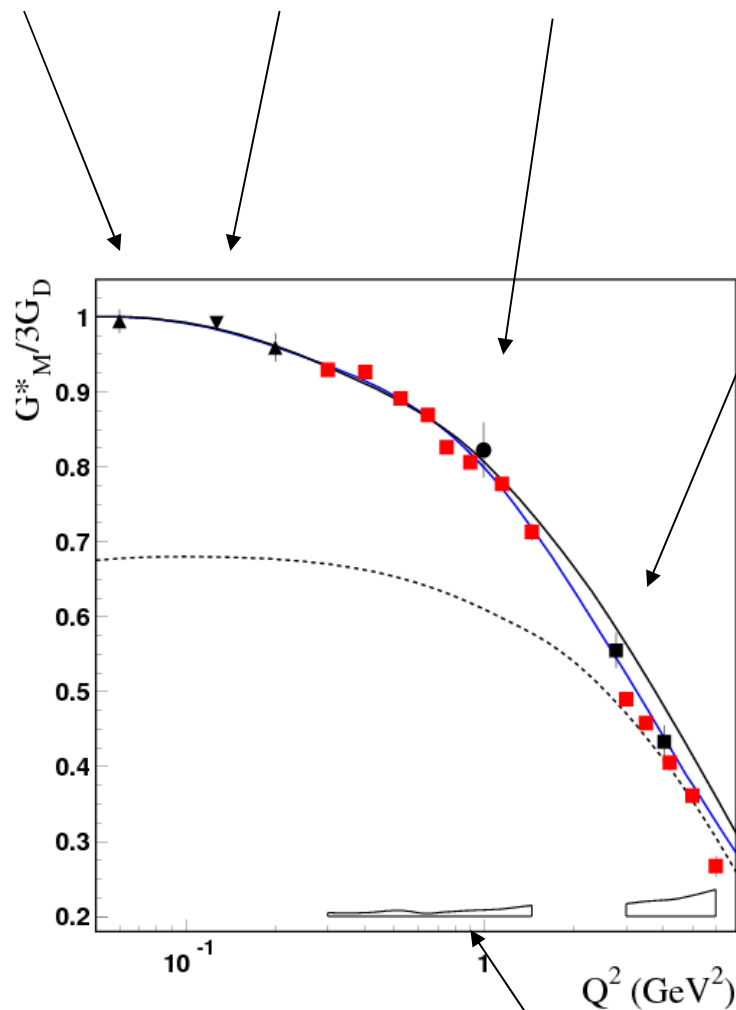
uncertainties due to the masses and widths of  $P_{11}(1440)$ ,  $D_{13}(1520)$ , and  $S_{11}(1535)$

**3.** Utilization of two approaches allowed us to estimate model dependence of the extracted electroexcitation amplitudes

# $P_{33}(1232)$

CLAS

MAMI MIT/Bates Jlab/Hall A Jlab/Hall C



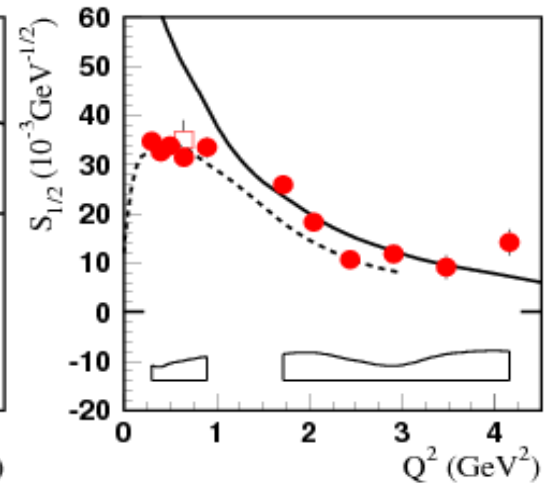
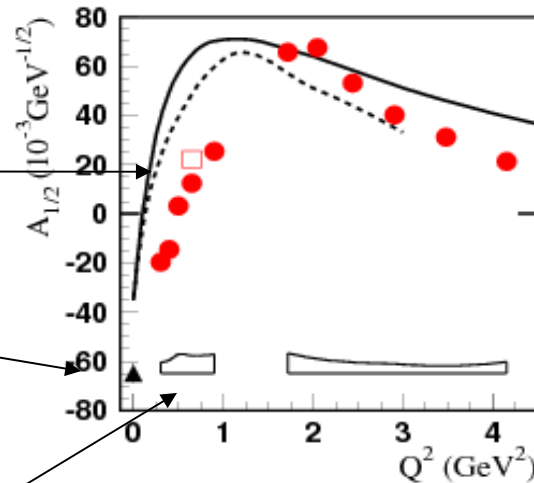
**Model uncertainties** = all uncertainties listed above added in quadrature

# Roper resonance $P_{11}(1440)$

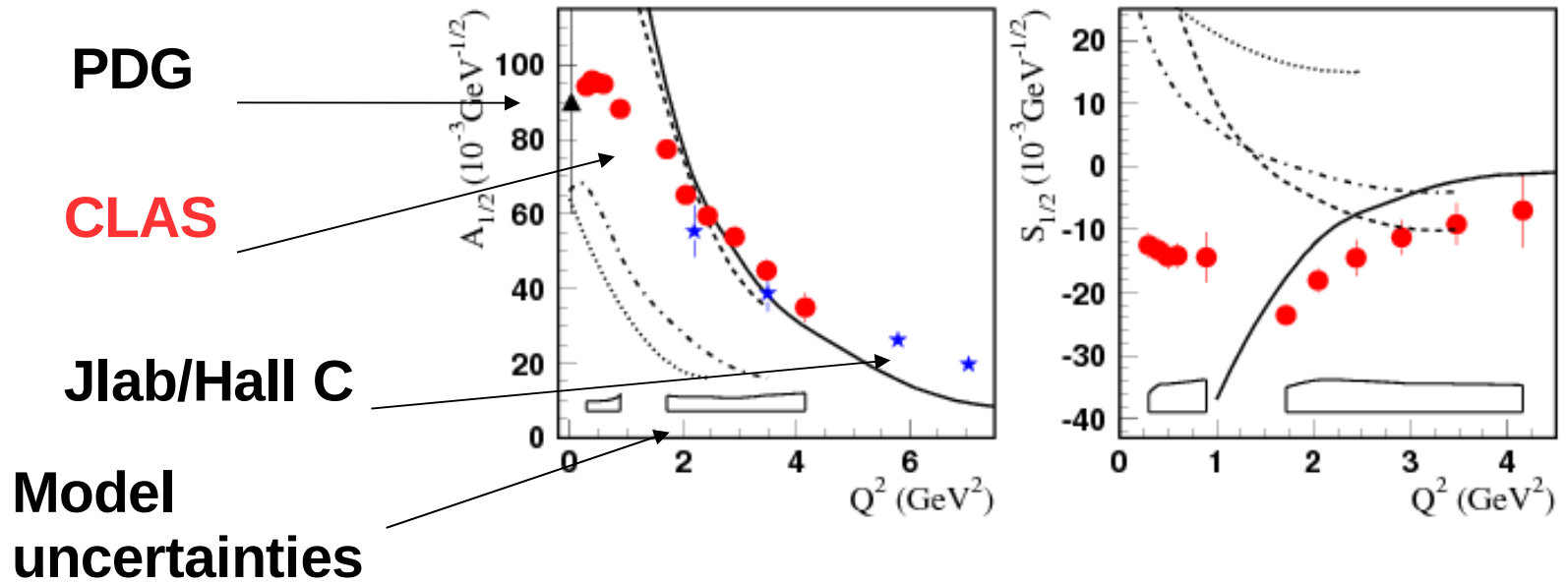
CLAS

PDG

Model  
uncertainties



# $S_{11}(1535)$

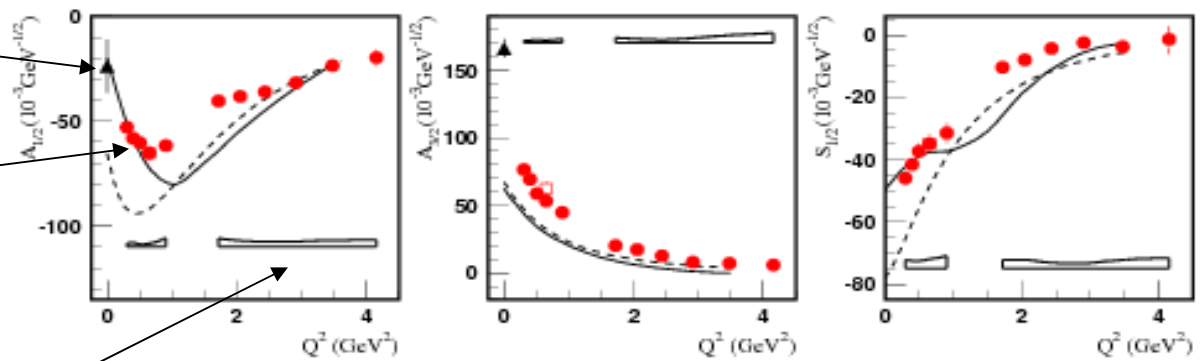


# $D_{13}(1520)$

PDG

CLAS

Model  
uncertainties



# Dispersion relations

---

The DR approach we use is presented in detail in:

Aznauryan, PR D57, 2727, 1998

Aznauryan, PR C67, 015209, 2003

Aznauryan, Burkert (CLAS Collaboration) PR C80, 055203, 2009

The process  $\gamma^* \mathbf{N} \rightarrow \mathbf{N} \pi$  is described by 18 invariant amplitudes  $\mathbf{B}_i^{(+,-,0)}(\mathbf{s}, \mathbf{t}, \mathbf{Q}^2)$ ,  $i=1, 2, \dots, 6$  which are defined in **gauge-invariant** form and have definite crossing symmetry according to replacements  $\mathbf{s} \rightarrow \mathbf{u}$ ,  $\mathbf{u} \rightarrow \mathbf{s}$ .

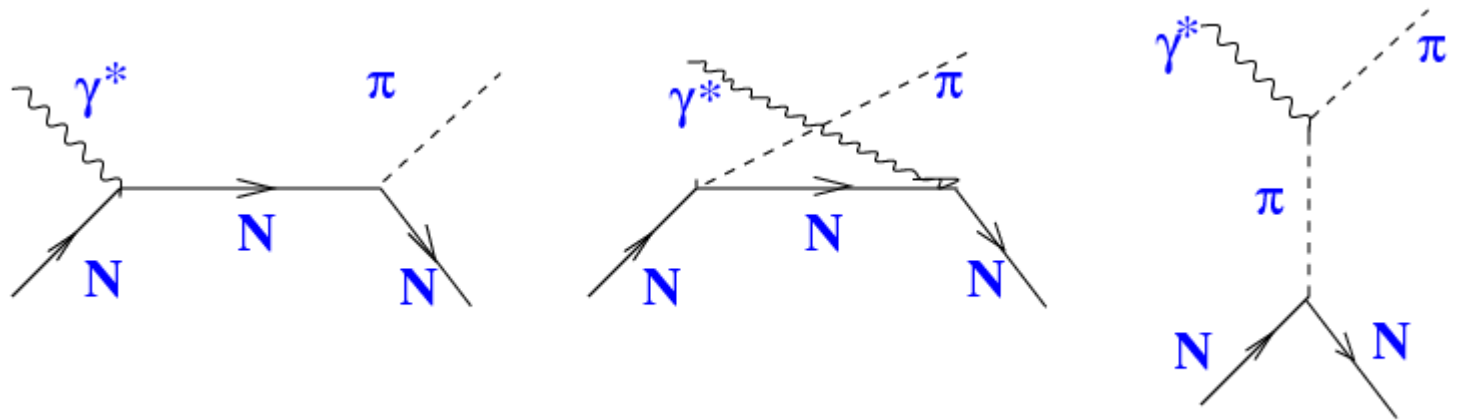
Using analytical properties of the amplitudes and their high energy Regge behaviour, for all these amplitudes, except  $\mathbf{B}_3^{(-)}(\mathbf{s}, \mathbf{t}, \mathbf{Q}^2)$ , unsubtracted dispersion relations at fixed  $\mathbf{t}$  can be written.  $\mathbf{B}_3^{(-)}(\mathbf{s}, \mathbf{t}, \mathbf{Q}^2)$  needs subtraction.

**DR determine real parts of amplitudes through integrals over their imaginary parts.**

**Re** $B_i(s, t, Q^2) =$  **Born term**

$$+\frac{1}{\pi} \int_{S_{\text{thr}}}^{\infty} \mathbf{Im}B_i(s', t, Q^2) \left( \frac{1}{s'-s} \pm \frac{1}{s'-u} \right) ds'$$

Born term:



$$\mathbf{Re}B_3^{(-)}(s, t, Q^2) = \mathbf{f}_{\text{sub}}(t, Q^2) - \mathbf{g}e \frac{F_\pi(Q^2)}{t-m_\pi^2}$$

$$- \frac{\mathbf{g}e}{4} [F_1^{\mathbf{P}}(Q^2) - F_1^{\mathbf{n}}(Q^2)] \left( \frac{1}{s-m^2} + \frac{1}{u-m^2} \right)$$

$$+\frac{\mathbf{P}}{\pi} \int_{S_{\text{thr}}}^{\infty} \mathbf{Im}B_3^{(-)}(s', t, Q^2) \left( \frac{1}{s'-s} + \frac{1}{s'-u} \right) ds'$$

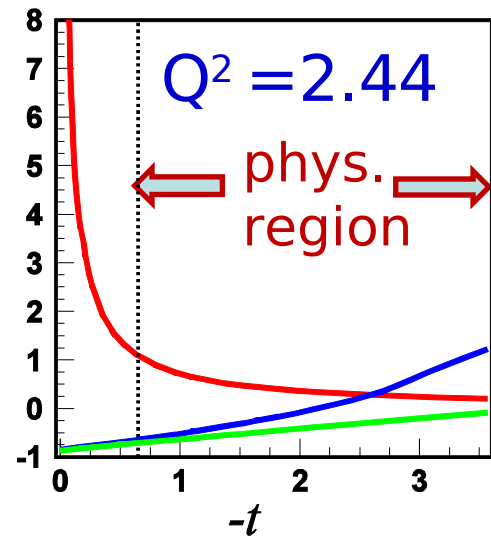
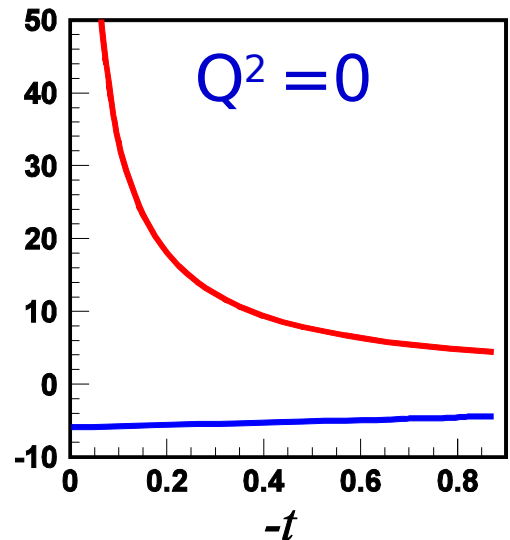
At  $Q^2 = 0$ , due to gauge invariance:

$$f_{\text{sub}}(\mathbf{t}) = 4 \frac{P}{\pi} \int_{s_{\text{thr}}}^{\infty} \frac{\text{Im} B_3^{(-)}(s', t, Q^2)}{u' - s'} ds' \quad (1)$$

At  $Q^2 = 0, 0.4, 0.65$ , (1) results in good description of the data

At  $Q^2 = 1.7 - 4.2$ ,  $f_{\text{sub}}$  was found from the fit to the data; subtractions at low and high  $Q^2$  are related smoothly

- $\pi$  contribution
- $f_{\text{sub}}(\mathbf{t})$  (1)
- $f_{\text{sub}}(\mathbf{t})$  from the fit



## Imaginary parts of amplitudes in the $P_{33}(1232)$ and $P_{11}(1440)$ , $D_{13}(1520)$ , and $S_{11}(1535)$ resonance regions

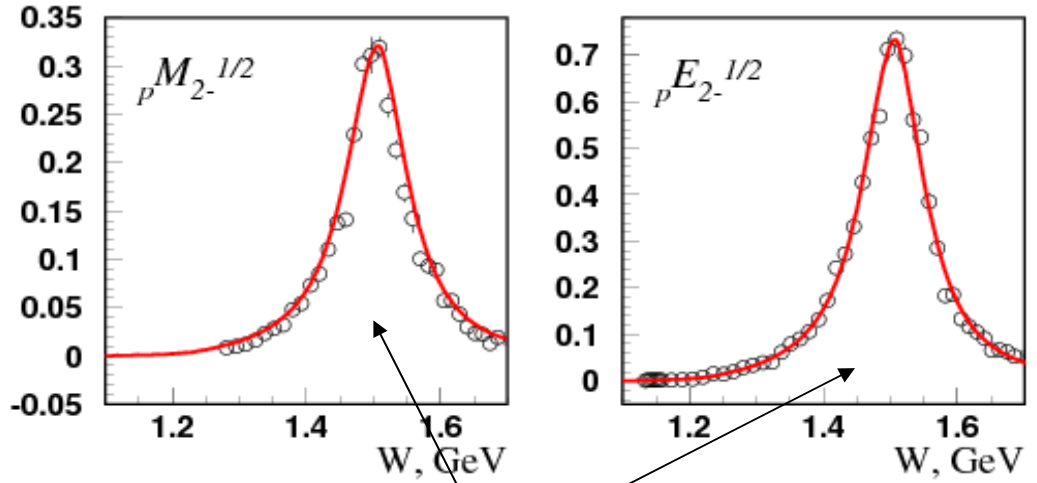
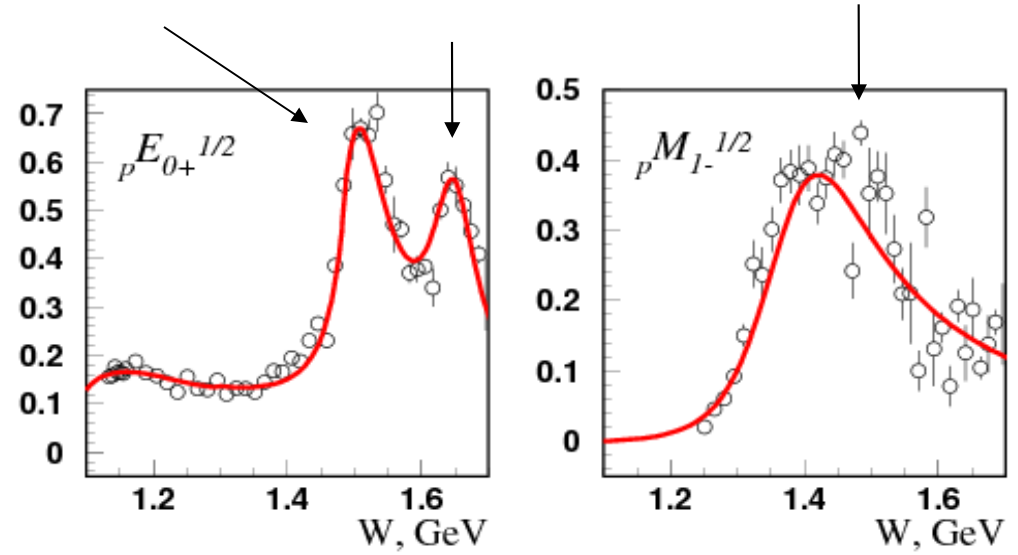
---

- 1.** The imaginary parts of the amplitudes  $M_{1+}^{(3/2)}$ ,  $E_{1+}^{(3/2)}$ ,  $S_{1+}^{(3/2)}$  that correspond to the  **$P_{33}(1232)$**  resonance were found from integral equations which follow from DR due to the Watson theorem and elasticity of the corresponding  $\pi N$  amplitude  $f_{1+}^{(3/2)}$ .
- 2.** Solutions of these equations for each of these amplitudes contain one parameter, which was found from the fit to the data

The **imaginary parts** of multipole amplitudes corresponding to the resonances  $P_{11}(1440)$ ,  $D_{13}(1520)$ , and  $S_{11}(1535)$  are determined mainly by **the resonance contributions.**

Examples at  $Q^2 = 0$   
Data from SAID

$S_{11}(1535)$     $S_{11}(1650)$     $P_{11}(1440)$



$D_{13}(1520)$

The contributions of  $P_{11}(1440)$ ,  $D_{13}(1520)$ , and  $S_{11}(1535)$ , as well as higher mass resonances, were taken in Breit-Wigner form with energy dependent widths.

Due to large phases of  $\pi N$  amplitudes  $f_{0+}^{(1/2)}$ ,  $f_{0+}^{(3/2)}$  near threshold, the imaginary parts of  $pE_{0+}^{(1/2)}$ ,  $E_{0+}^{(3/2)}$ ,  $pS_{0+}^{(1/2)}$ ,  $S_{0+}^{(3/2)}$  have significant non-resonant parts below  $W=1.3$  GeV. They were found in the following way:

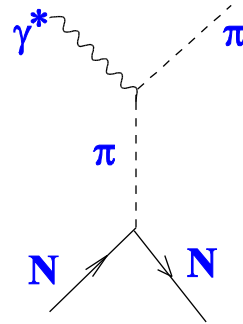
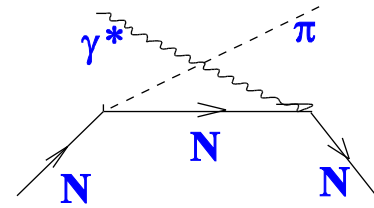
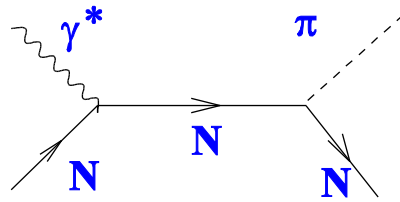
- (i) We found real parts of these amplitudes using DR
- (ii) Then their imaginary parts were built using the Watson theorem
- (iii) At higher energies these contributions were smoothly reduced to 0

# Unitary Isobar Model

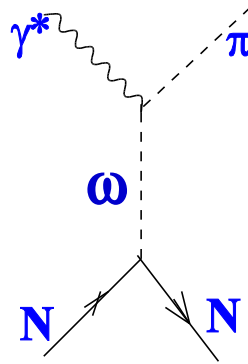
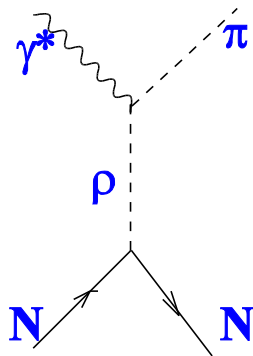
Our UIM is based on Mainz UIM (MAID); the modifications will be discussed below

**Non-resonant background consists from:**

Born term with mixed PS-PV coupling in  $\pi NN$  vertex



and t-channel  $\rho$  and  $\omega$  contributions



With increasing  $W$ , some multipole amplitudes, obtained with this background, become too large and strongly disagree with the data.

For this reason MAID introduces energy-dependent phases in resonance contributions to compensate large background.

We, in contrary, describe all resonance contributions with the unified Breit-Wigner parametrization, but modify background by linking it to the high-energy Regge-pole amplitudes:

**At  $s < s_0$**       Background =  $[N + \pi + \rho + \omega]_{\text{UIM}}$

**At  $s > s_0$**       Background =

$$= [N + \pi + \rho + \omega]_{\text{UIM}} \frac{1}{1 + (s - s_0)^2} +$$
$$\text{Re}[\pi + \rho + \omega + b_1 + a_2]_{\text{Regge}} \frac{(s - s_0)^2}{1 + (s - s_0)^2}.$$

Good description of the data below  $Q^2 = 0.65 \text{ GeV}^2$  was obtained with  $s_0 = 1.2 \text{ GeV}^2$ . At high  $Q^2$  and  $W < 1.7 \text{ GeV}$ , the incorporation of the Regge poles was unnecessary.

As in MAID, background was unitarized in the K-matrix approximation. Unitarization was made for each multipole amplitude:

$$M_{l\pm} = M_{l\pm}^{\text{back}} (1 + i f_{l\pm}^{\pi N})$$

For the purposes of this Workshop we present multipole amplitudes obtained within DR and UIM:

multipole amplitudes are the quantities which are more directly related to the observables

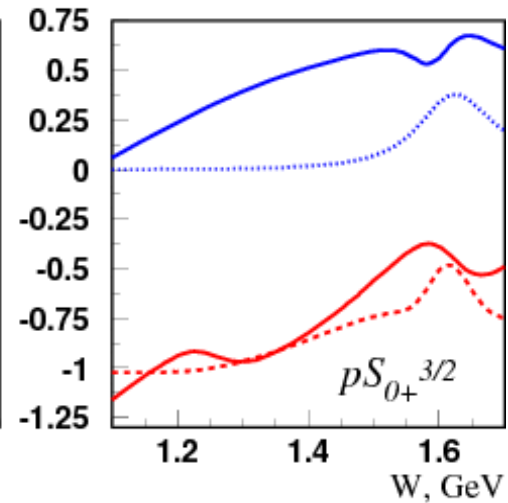
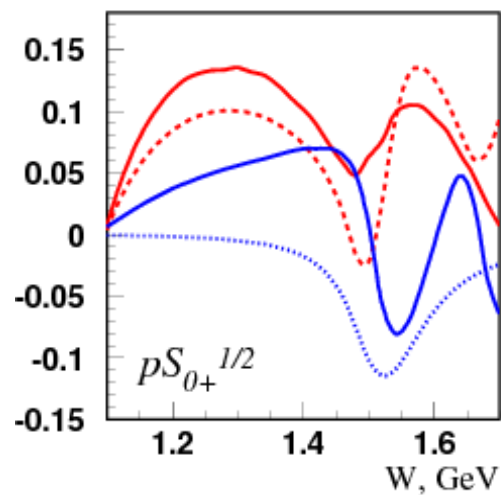
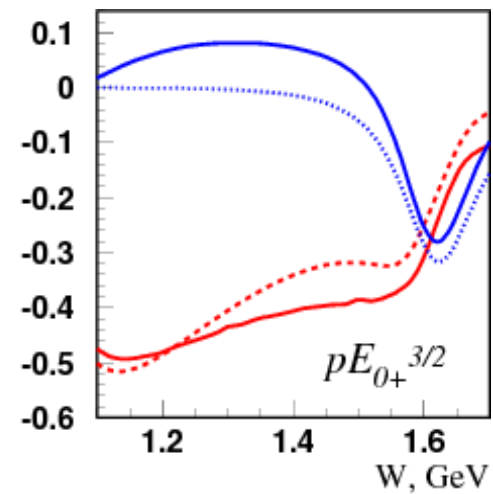
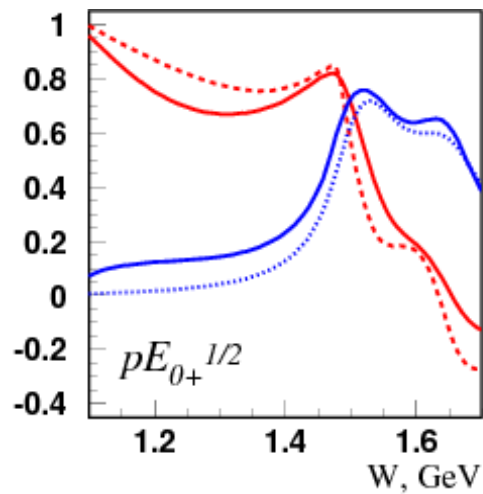
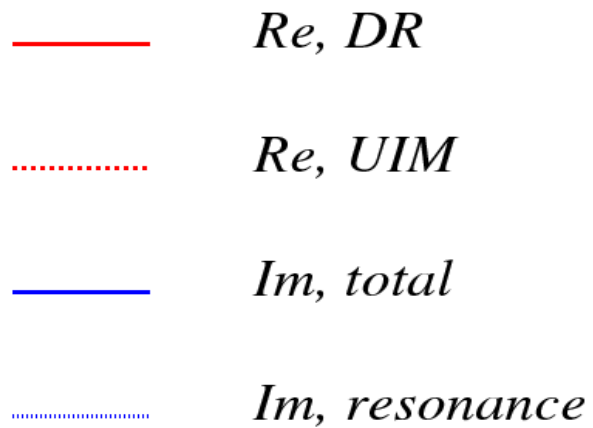
in terms of multipole amplitudes we can in clear way show the resonant and non-resonant contributions

multipole amplitudes allow one to make direct comparison between approaches

The imaginary parts of amplitudes in DR and UIM are close to each other. The difference is more visible in real parts.

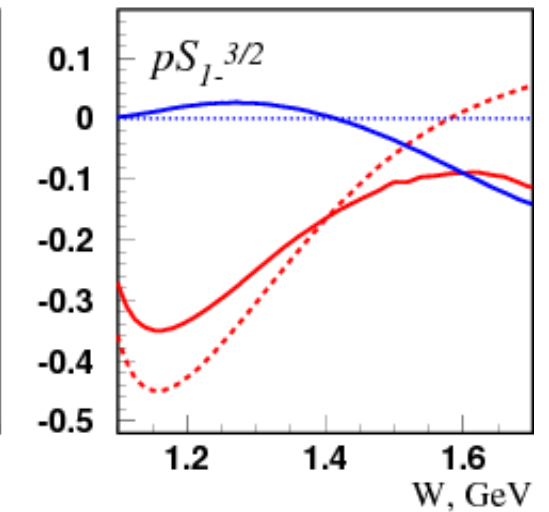
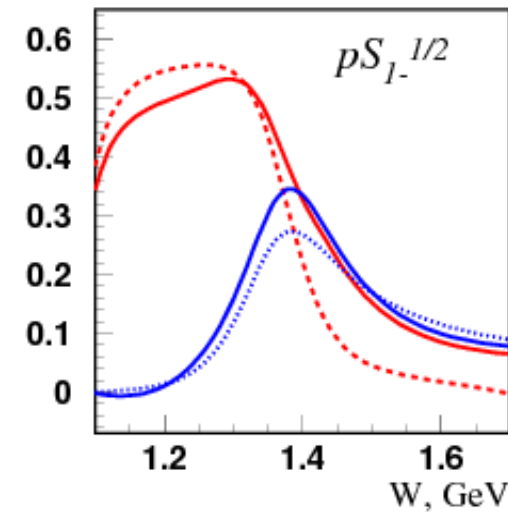
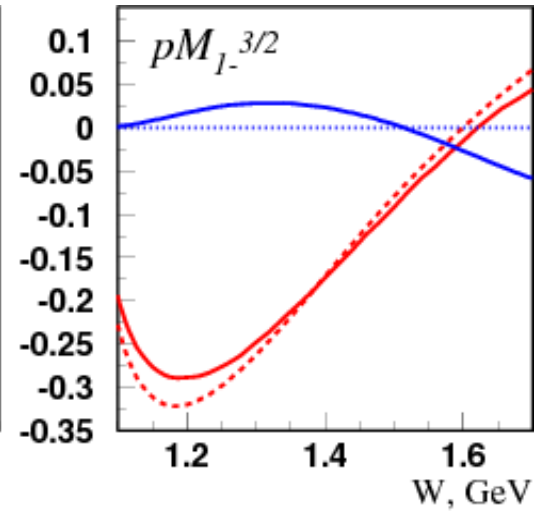
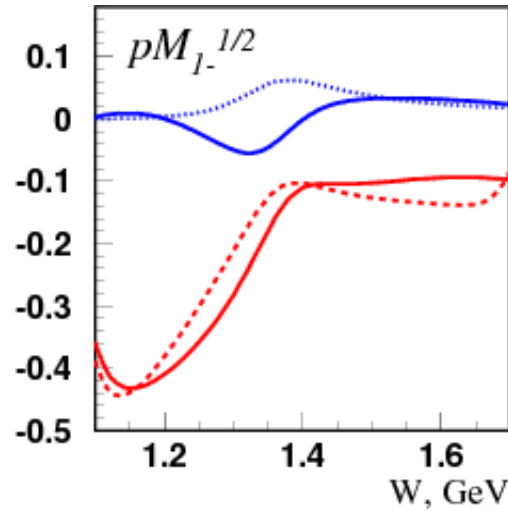
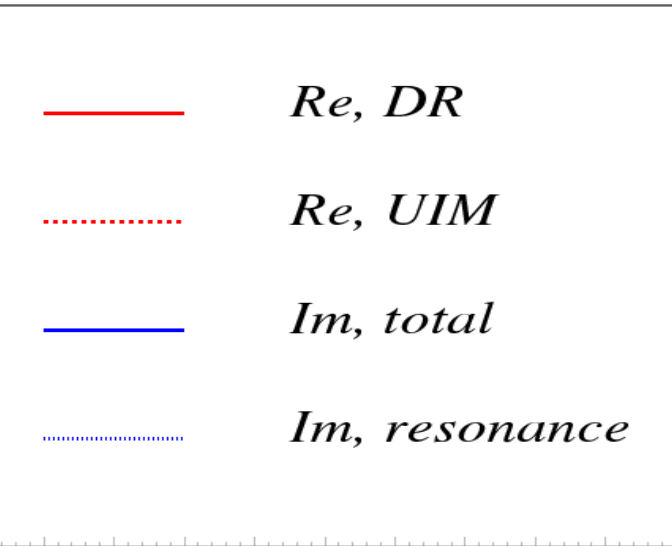
To get more clear understanding of these differences, we constructed real parts of multipole amplitudes supposing identical imaginary parts, which are taken as mean values of those in DR and UIM.

$Q^2 = 0.4 \text{ GeV}^2$



All amplitudes are in  $(\text{mkb})^{1/2}$  units

$Q^2 = 0.4 \text{ GeV}^2$



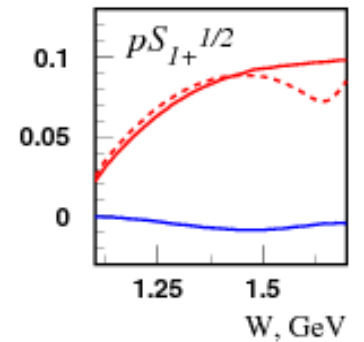
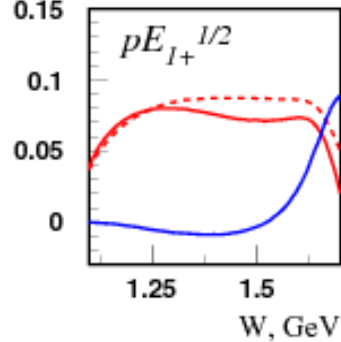
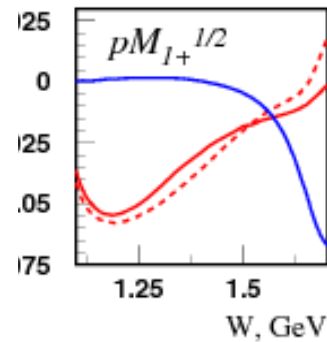
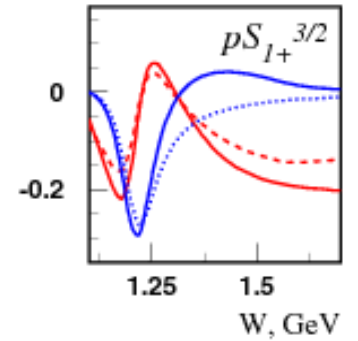
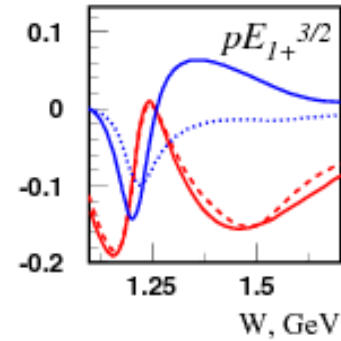
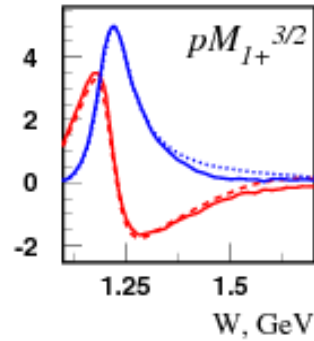
$$Q^2 = 0.4 \text{ GeV}^2$$

—  $Re, DR$

⋯  $Re, UIM$

—  $Im, total$

⋯  $Im, resonance$



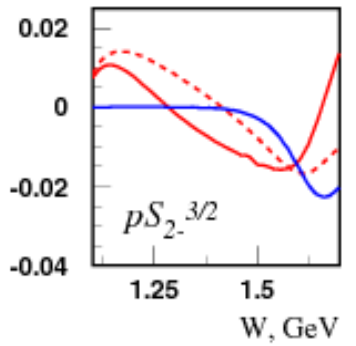
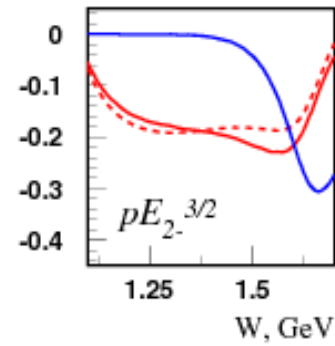
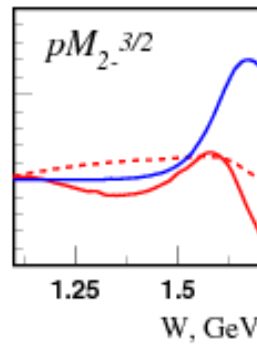
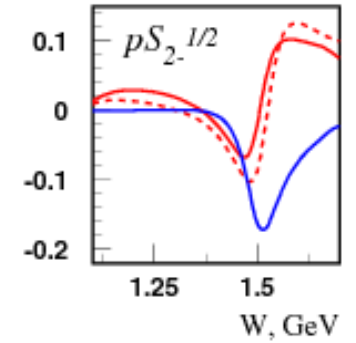
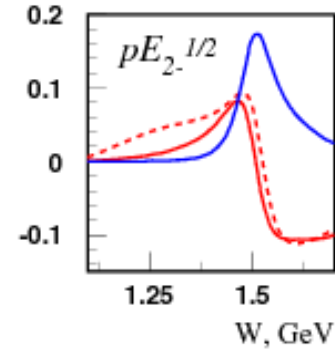
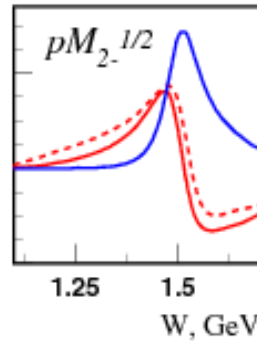
$$Q^2 = 0.4 \text{ GeV}^2$$

—  $Re, DR$

- - -  $Re, UIM$

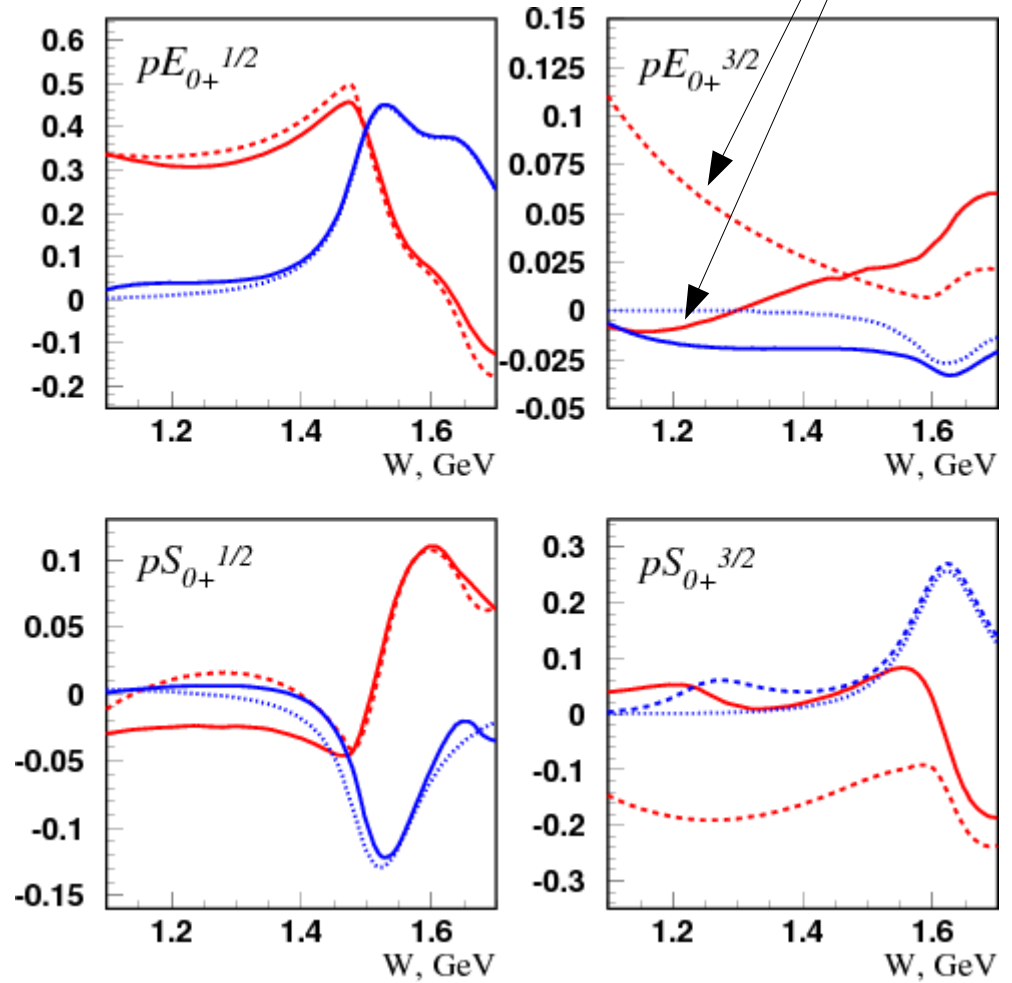
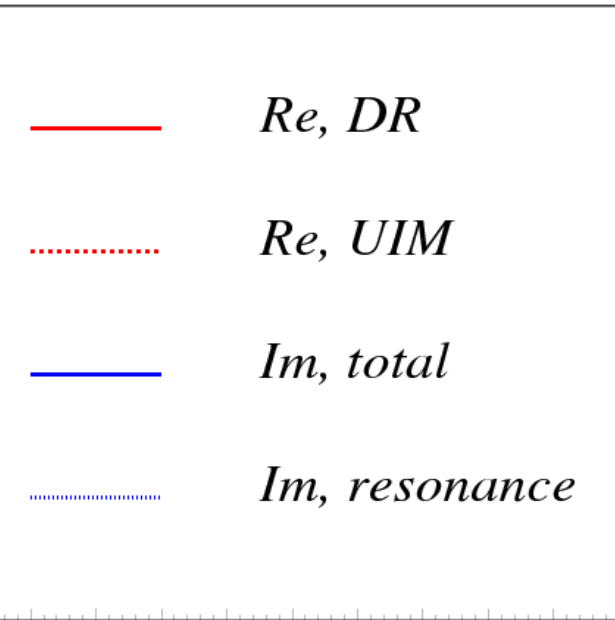
—  $Im, total$

⋯  $Im, resonance$

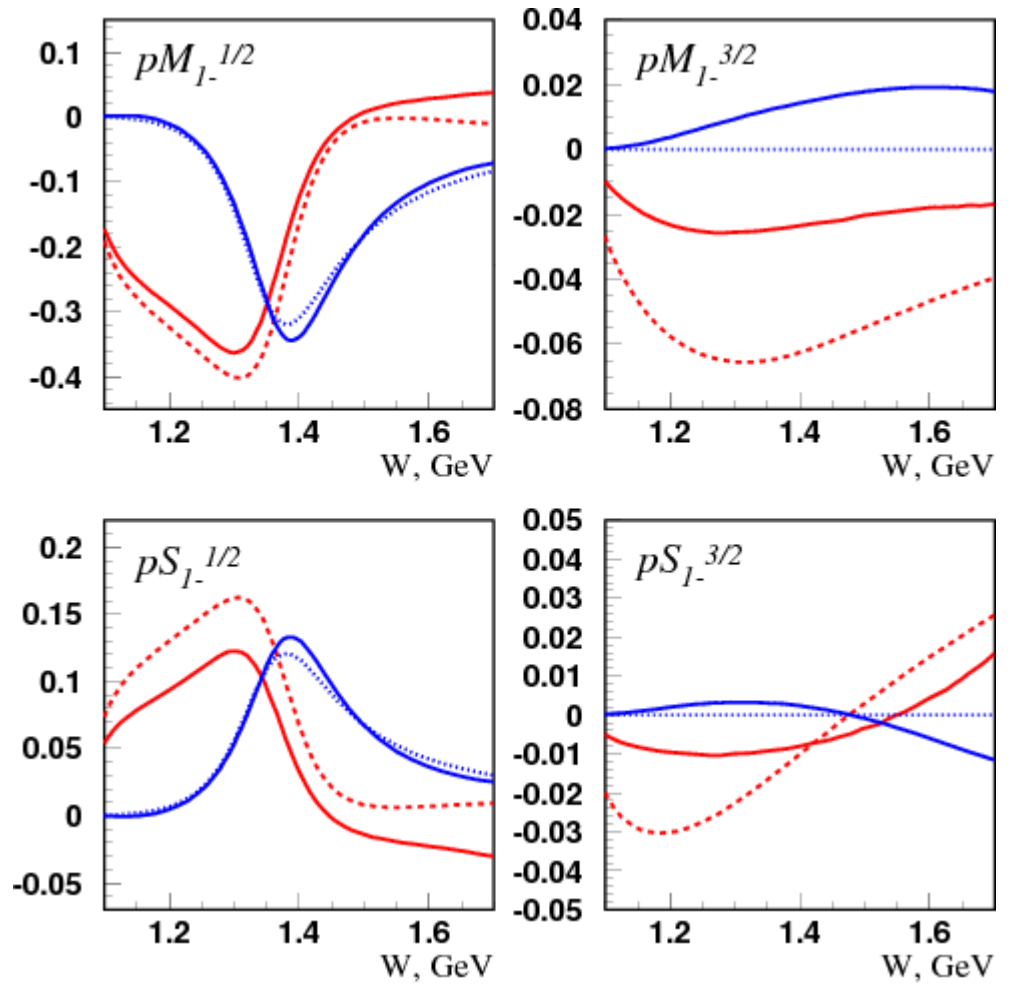
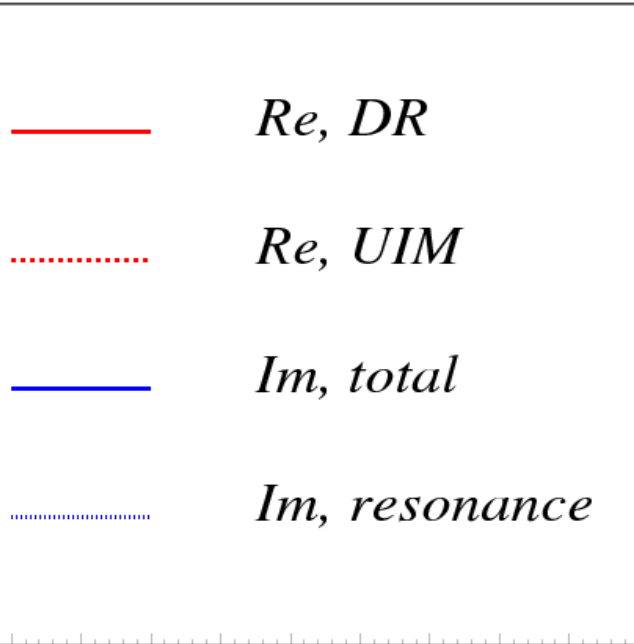


$Q^2 = 2.5 \text{ GeV}^2$

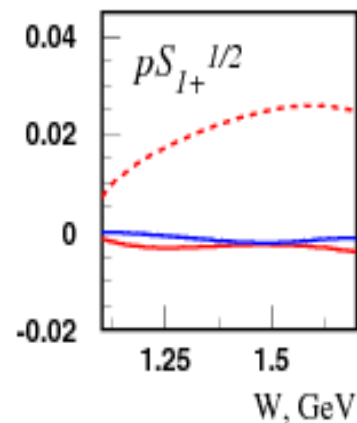
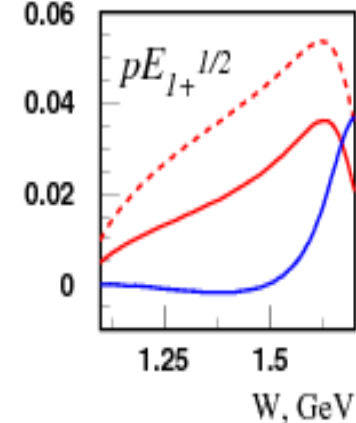
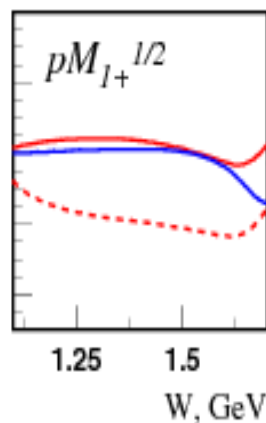
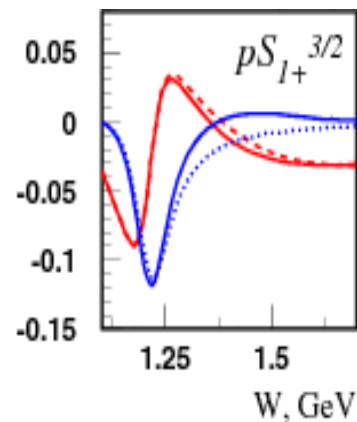
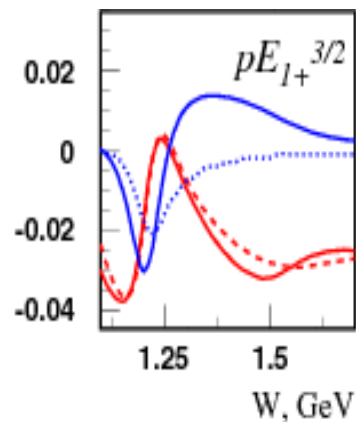
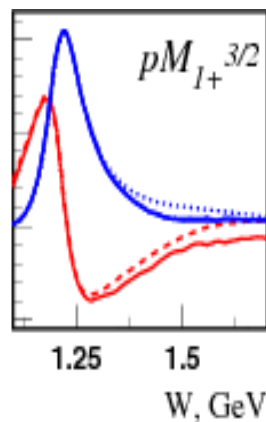
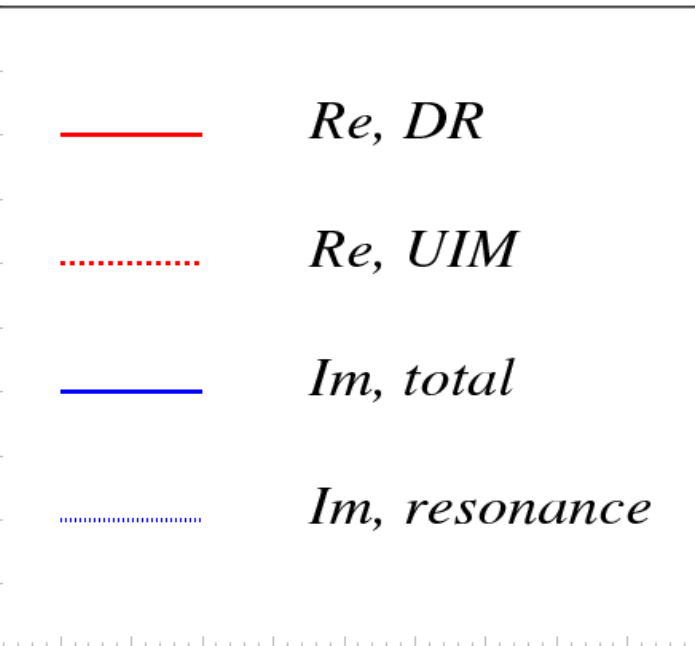
Difference, which we will discuss in conclusion



$Q^2 = 2.5 \text{ GeV}^2$



$Q^2 = 2.5 \text{ GeV}^2$



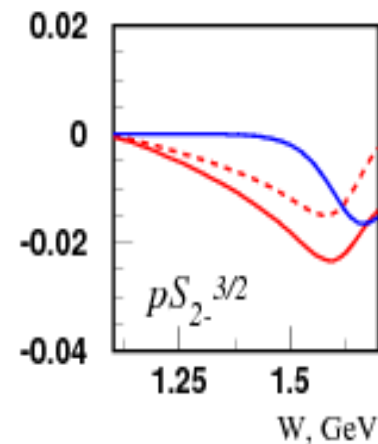
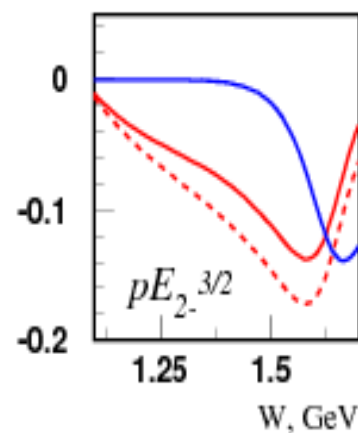
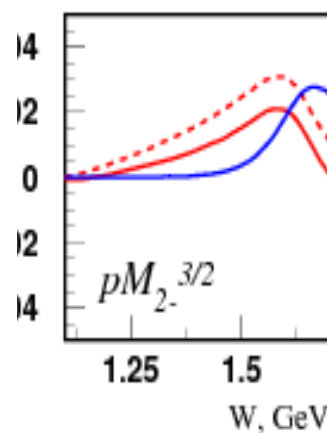
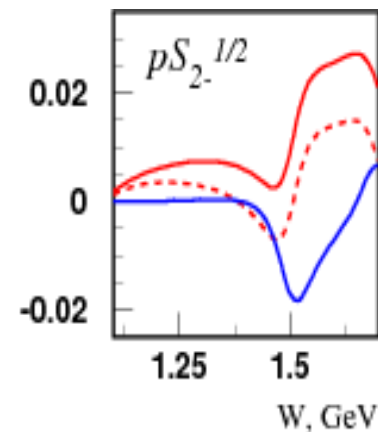
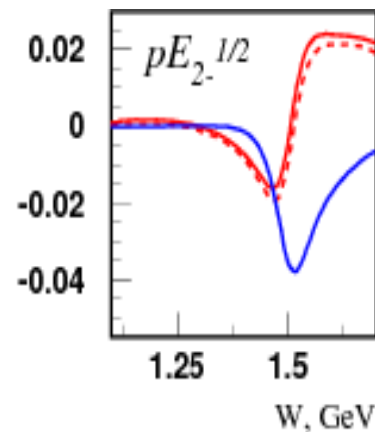
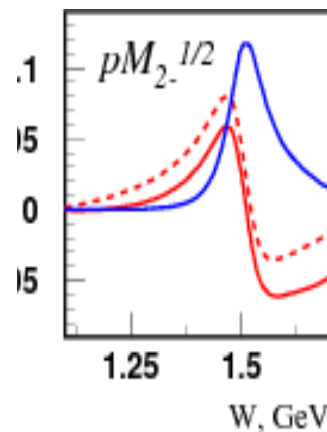
$$Q^2 = 2.5 \text{ GeV}^2$$

—  $Re, DR$

⋯  $Re, UIM$

—  $Im, total$

⋯  $Im, resonance$



## Some conclusions:

At low  $Q^2$ , DR and UIM give close results for the multipole amplitudes.

With increasing  $Q^2$ , there are some inconsistencies between amplitudes obtained within DR and UIM.

Let us remind that the results for the electroexcitation amplitudes obtained in our analysis of all CLAS data (PR C80, 055203, 2009) are mean values of those extracted using DR and UIM.

**It is very important to analyze the data using different approaches in order to be able to make conclusions on the model sensitivity of the results.**

**On the difference between DR and UIM results for  $E_{0+}^{(3/2)}$  at high  $Q^2$  near threshold.**

**It can be checked by experiment near threshold:**

$$\frac{\sigma(\gamma^* \mathbf{p} \rightarrow \pi^+ \mathbf{n})}{\sigma(\gamma^* \mathbf{p} \rightarrow \pi^0 \mathbf{p})} \simeq \mathbf{2} \quad \text{for DR}$$

$$\frac{\sigma(\gamma^* \mathbf{p} \rightarrow \pi^+ \mathbf{n})}{\sigma(\gamma^* \mathbf{p} \rightarrow \pi^0 \mathbf{p})} < \mathbf{1} \quad \text{for UIM and MAID}$$